

# Make a suitable title: my paper on the cosmic microwave background and formation of structures in our Universe

V. A. Vikenes<sup>1</sup>

Institute of Theoretical Astrophysics, University of Oslo, 0315 Oslo, Norway  
e-mail: v.a.vikenes@astro.uio.no

March 4, 2023

## ABSTRACT

An abstract for the paper. Describe the paper. What is the paper about, what are the main results, etc.

**Key words.** cosmic microwave background – large-scale structure of Universe

## 1. Introduction

Write an introduction here. Give context to the paper. Citations to relevant papers. You only need to do this in the end for the last milestone.

## 2. Milestone I

In this section we want to study the evolution of the uniform background in the Universe. Our main goal of this section will be to implement methods that computes the Hubble parameter, as well as related time- and distance measures **Rewrite**. To do this, we will solve **simple** ordinary differential equations (ODEs) numerically. For the fiducial cosmology we will use results from the Planck Collaboration [1]. We will then test our implementation with known theoretical solutions, to assess the validity of our methods.

The main goal of this section is mainly concerned with using known parameter values to **predict/solve** the background cosmology. Another interesting aspect is to use data to constrain such cosmological parameters. To do this, we will use data from supernova observations [2], containing luminosity distance associated with different values of redshift. Implementing our solver, we will implement a simple Markov chain Monte Carlo (MCMC) algorithm, in order to estimate the best fits of  $h$ ,  $\Omega_m$  and  $\Omega_\Lambda$ , which are the Hubble parameter, and the density parameter of matter and dark energy, respectively.

### 2.1. Theory

The theory behind this milestone. **Define ALL parameters**  
**Neutrinos are on the loose. Catch them before it's too late.**  
**Define most important stuff here**

#### 2.1.1. Density parameters

The Friedmann equation can be written in terms of density parameters,  $\Omega_i \equiv \rho_i/\rho_c$ , where  $\rho_c \equiv 3H^2/8\pi G$  is the critical density. We will assume that a given species,  $i$ , of the Universe can be described by a constant equation of state,  $w_i \equiv P_i/\rho_i$ , where

$P_i$  denotes the pressure. The density of a species evolves as [3, Eq. (2.72)]

$$\rho_i(t) \propto a(t)^{-3(1+w_i)}. \quad (1)$$

For baryons and cold dark matter (CDM), we have  $w = 0$ , for photons and massless neutrinos (**Write massless assumption**) we have  $w = 1/3$  and for a cosmological constant we have  $w = -1$ . Including a curvature parameter  $\Omega_k$ , with  $w = -1/3$ , the Friedmann Equation can be written as [3, Eq. (3.14)]

$$H = H_0 \sqrt{\Omega_{m0}a^{-3} + \Omega_{r0}a^{-4} + \Omega_{k0}a^{-2} + \Omega_{\Lambda0}}, \quad (2)$$

where  $H \equiv \dot{a}/a$  is the Hubble parameter, with the dot denoting a derivative with respect to cosmic time,  $t$ . For brevity, we have expressed the density parameters of matter and radiation as  $\Omega_{m0} = \Omega_{b0} + \Omega_{\text{CDM}0}$  and  $\Omega_{r0} = \Omega_{\gamma0} + \Omega_{\nu0}$ , respectively. A subscript 0 indicates the value of a given parameter today, at  $a = 1$ . The density parameters of radiation follow from the CMB temperature, and are given by

$$\Omega_{\gamma0} = 2 \cdot \frac{\pi^2}{30} \frac{(k_b T_{\text{CMB}0})^4}{\hbar^3 c^5} \cdot \frac{8\pi G}{3H_0^2}, \quad (3)$$

$$\Omega_{\nu0} = N_{\text{eff}} \cdot \frac{7}{8} \cdot \left(\frac{4}{11}\right)^{4/3} \Omega_{\gamma0}. \quad (4)$$

The value of  $\Omega_{\Lambda0}$  is fixed by the requirement that  $H(a = 1) = H_0$ , yielding

$$\Omega_{\Lambda0} = 1 - (\Omega_{m0} + \Omega_{r0} + \Omega_{k0}). \quad (5)$$

We also introduce the scaled Hubble factor,  $\mathcal{H} \equiv aH$ . Rather than working with the scale factor,  $a(t)$ , we will mainly be working with the logarithm of the scale factor

$$x \equiv \ln a, \quad ' \equiv \frac{d}{dx}. \quad (6)$$

The resulting expression for  $\mathcal{H}(x)$  is thus

$$\mathcal{H}(x) = H_0 \sqrt{\Omega_{m0}e^{-x} + \Omega_{r0}e^{-2x} + \Omega_{k0} + \Omega_{\Lambda0}e^{2x}}. \quad (7)$$

Once  $\mathcal{H}(x)$  is known, we can compute the value of the density parameters at any given  $x$ , with

$$\Omega_k(x) = \frac{\Omega_{k0}}{\mathcal{H}(x)^2/H_0^2}, \quad (8)$$

$$\Omega_m(x) = \frac{\Omega_{m0}}{e^x \mathcal{H}(x)^2/H_0^2}, \quad (9)$$

$$\Omega_r(x) = \frac{\Omega_{r0}}{e^{2x} \mathcal{H}(x)^2/H_0^2}, \quad (10)$$

$$\Omega_\Lambda(x) = \frac{\Omega_{\Lambda 0}}{e^{-2x} \mathcal{H}(x)^2/H_0^2}, \quad (11)$$

With these expressions, we can determine when the Universe was dominated by an equal amount of matter and radiation, and by an equal amount of matter and cosmological constant. These can be found numerically, as  $\Omega_r(x) = \Omega_m(x)$  and  $\Omega_m(x) = \Omega_\Lambda(x)$ , respectively. Another time of interest is the onset of acceleration, defined as the time when  $\ddot{a} = 0$ . In terms of  $\mathcal{H}$  and  $x$ , this corresponds to

$$\ddot{a} = \frac{dx}{dt} \frac{da}{dx} = \frac{d \ln a}{dt} \frac{d\mathcal{H}(x)}{dx} = e^{-x} \mathcal{H}(x) \frac{d\mathcal{H}(x)}{dx}. \quad (12)$$

In Sect. 2.1.4 we will derive an expression for the derivative of  $\mathcal{H}$  that we can use.

### 2.1.2. Conformal time

Having considered the main quantities governing the evolution of the background cosmology in terms of  $x$ , we want to relate these quantities to some time variables. One of the main time variables we will be working with is the conformal time,  $\eta$ , which is a measure of the distance light have been able to travel since  $t = 0$ , where  $t$  is the cosmic time. Using its definition in terms of  $t$  [3, Eq. (2.90)], we can express it in terms of  $x$  as

$$\eta = \int_0^t \frac{c dt'}{a(t')} = \int_{-\infty}^x \frac{c dx'}{\mathcal{H}(x')}. \quad (13)$$

This leads us to the following differential equation that we will solve numerically

$$\frac{d\eta}{dx} = \frac{c}{\mathcal{H}(x)}. \quad (14)$$

The initial condition we have is  $\eta(-\infty) = 0$ . Noting from Eq. (7) that  $\mathcal{H}(x) \rightarrow H_0 \sqrt{\Omega_{r0}} e^{-x}$  as  $x \rightarrow -\infty$ , we get an analytical approximation for the initial condition of  $\eta$  at early times

$$\eta(x_{\text{start}}) \approx \int_{-\infty}^{x_{\text{start}}} \frac{c dx'}{H_0 \sqrt{\Omega_{r0}}} e^{x'} = \frac{c}{\mathcal{H}(x_{\text{start}})}. \quad (15)$$

**Move sentence below to check section.** From this, we also get a way of checking that our solution is reasonable, by checking if  $\eta(c)\mathcal{H}(x)/c = 1$  at low  $x$ .

In addition to  $\eta$ , we also want to know the value of  $t$  at different points in the Universe's evolution. By definition,  $H = \dot{a}/a$ , and from the chain rule we obtain a differential equation for  $t(x)$  which we can solve numerically,

$$\frac{dt}{dx} = \frac{1}{H(x)}. \quad (16)$$

To get an initial condition for  $t$ , we consider the radiation dominating era, with the following integral expression

$$t(x) = \int_{-\infty}^x \frac{dx'}{H(x')}. \quad (17)$$

Comparing with Eq. (15), we see that the two integrands only differ by a factor  $e^x$ . The initial condition for  $t$  is therefore easily seen to be

$$t(x_{\text{start}}) = \frac{1}{2H(x_{\text{start}})}. \quad (18)$$

### 2.1.3. Distance measures

**Rewrite this, express with x.**

For the supernova fitting, we will need a measure of the luminosity distance,  $d_L$ , defined as

$$d_L(a) = \frac{d_A}{a^2} = \frac{r}{a}, \quad (19)$$

where  $d_A = ar$  is the angular distance of the source at a distance  $r$  away from us. Photons move on 0-geodesics, and from the line element in spherical coordinates,

$$ds^2 = -c^2 dt^2 + a^2 \left( \frac{dr^2}{1 - kr^2} + r^2 d\theta^2 + r^2 \sin^2 \theta d\phi^2 \right), \quad (20)$$

we get the co-moving distance by integrating the line element of radially moving photons. For a photon emitted at,  $(t, r)$ , reaching an observer at  $(t_0, 0)$ , we get

$$\int_0^r \frac{dr'}{\sqrt{1 - kr'}} = \int_t^{t_0} \frac{c dt}{a}. \quad (21)$$

**(Define  $\Omega_{k0} = -kc^2/H_0^2$ )**

The RHS is the co-moving distance,  $\chi$ , which in terms of conformal time is given as

$$\chi = \int_t^{t_0} \frac{c dt}{a} = \int_x^0 \frac{c dx'}{\mathcal{H}(x')} = \eta(0) - \eta(x). \quad (22)$$

Solving Eq. (21) with respect to  $r$ , we get **(check punctuation after cases)**

$$r = \begin{cases} \chi \cdot \frac{\sin(\sqrt{|\Omega_{k0}|} H_0 \chi / c)}{(\sqrt{|\Omega_{k0}|} H_0 \chi / c)}, & \Omega_{k0} < 0 \\ \chi, & \Omega_{k0} = 0 \\ \chi \cdot \frac{\sinh(\sqrt{|\Omega_{k0}|} H_0 \chi / c)}{(\sqrt{|\Omega_{k0}|} H_0 \chi / c)}, & \Omega_{k0} > 0 \end{cases} \quad (23)$$

### 2.1.4. Analytical solutions (Working title)

In order to test our solutions we will need the first and second derivative of  $\mathcal{H}(x)$ . To simplify the resulting expressions, we define the function,  $g(x)$ , as the derivative of the term inside the square root in Eq. (7), namely

$$g(x) \equiv -\Omega_{m0} e^{-x} - 2\Omega_{r0} e^{-2x} + 2\Omega_{\Lambda 0} e^{2x}. \quad (24)$$

The first two derivatives of  $\mathcal{H}(x)$  are

$$\frac{d\mathcal{H}(x)}{dx} = \frac{H_0^2}{2\mathcal{H}(x)} g(x), \quad (25)$$

$$\frac{d^2\mathcal{H}(x)}{dx^2} = \frac{H_0^2}{2\mathcal{H}(x)} \left[ g'(x) - \frac{1}{2} \left( \frac{H_0 g(x)}{\mathcal{H}(x)} \right)^2 \right]. \quad (26)$$

Now we will consider the situation where the Universe is dominated by a single fluid with a constant equation of state parameter,  $w$ . The density of that fluid evolves according to (1), which we express in terms of the Hubble parameter,

$$H(t)^2 \propto a^{-3(1+w)} \implies \mathcal{H}(x) = c_1 e^{-\frac{3}{2}(1+w)x}, \quad (27)$$

where  $c_1$  is some constant. Now we obtain an analytical expression for  $\mathcal{H}'(x)/\mathcal{H}(x)$  in terms of  $w$  only, as other factors cancel out. Using that  $w = 1/3, 0, -1$  for radiation, matter and the cosmological constant, we get

$$\frac{1}{\mathcal{H}(x)} \frac{d\mathcal{H}}{dx} = -\frac{1+3w}{2} = \begin{cases} -1, & w = 1/3 \\ -1/2, & w = 0 \\ 1, & w = -1 \end{cases} \quad (28)$$

Similarly, the expression for  $\mathcal{H}''(x)/\mathcal{H}(x)$  becomes

$$\frac{1}{\mathcal{H}(x)^2} \frac{d^2\mathcal{H}}{dx^2} = \frac{(1+3w)^2}{2} = \begin{cases} 1, & w = 1/3 \\ 1/4, & w = 0 \\ 1, & w = -1 \end{cases} \quad (29)$$

Equations (28) and (29) offer a means to evaluate the accuracy of our numerical solution. By computing the values of  $\mathcal{H}$ ,  $\mathcal{H}'$ , and  $\mathcal{H}''$ , we can examine whether these quantities exhibit the expected behaviour in regimes where a single component dominates the Universe. This allows us to assess the validity of our model and ensure that it is consistent with the underlying physical principles.

## 2.2. Implementation details

Something about the numerical work.

### 2.2.1. Splining and data analysis (Working title)

When working

### 2.2.2. MCMC (Working title)

The supernova data we will use contains  $N = 31$  data points of luminosity distance,  $d_L^{\text{obs}}(z_i)$ , with associated measurement errors,  $\sigma_i$ , at different redshifts,  $z_i \in [0.01, 1.30]$ . Using these measurements, we want to constrain the three-dimensional parameter space

$$C = \{\hat{h}, \hat{\Omega}_{m0}, \hat{\Omega}_{k0}\}, \quad (30)$$

where the hat is used to distinguish them from the fiducial values. **Fiducial?**

We will assume that the measurements at different redshifts are normal distributed and uncorrelated. The likelihood function is then given by  $L \propto e^{-\chi^2/2}$ , where

$$\chi^2(C) = \sum_{i=1}^N \frac{[d_L(z_i, C) - d_L^{\text{obs}}(z_i)]^2}{\sigma_i^2}, \quad (31)$$

is the function we want to minimize. **Little h needs to be defined.** To do this, we will sample parameter values randomly by a MCMC process. The parameter space we will explore is limited to

$$\begin{aligned} 0.5 < \hat{h} < 1.5, \\ 0 < \hat{\Omega}_{m0} < 1, \\ -1 < \hat{\Omega}_{k0} < 1. \end{aligned} \quad (32)$$

To generate a new sample, we update each parameter by generating a random number  $P \sim \mathcal{N}(0, 1)$ , and multiplying it by a step size. We will use step sizes of  $\Delta\hat{h} = 0.007$ ,  $\Delta\hat{\Omega}_{m0} = 0.05$ ,  $\Delta\hat{\Omega}_{k0} = 0.05$ . To determine whether a new configuration should be included in the sample we use the Metropolis algorithm, where we always accept a state if it yields a lower value of  $\chi^2$  compared to the previous state that was accepted. If the new value of  $\chi^2$  is greater than the old one, we accept it if the ratio of the likelihood functions  $L(\chi_{\text{new}}^2)/L(\chi_{\text{old}}^2) > p$ , where  $p \sim \mathcal{U}(0, 1)$ . We continue drawing samples until we get a total of  $\hat{n} = 10^4$  samples. For the samples generated, we omit the first 1000 samples of the chain from our analysis.

With our generated samples, we can use the best fit,  $\chi_{\text{min}}^2$ , to find the  $1\sigma$  and  $2\sigma$  confidence regions. For the  $\chi^2$  distribution with 3 parameters, these regions are given by  $\chi^2 - \chi_{\text{min}}^2 < 3.53$  and  $\chi^2 - \chi_{\text{min}}^2 < 8.02$ , respectively. We will plot the  $1\sigma$  and  $2\sigma$  constraint in the  $(\Omega_{m0}, \Omega_{\Lambda0})$  plane. Since  $\Omega_{r0} < 10^{-4}$ ,  $\Omega_{\Lambda0}$  can be approximated well by  $\Omega_{\Lambda0} = 1 - \Omega_{m0}$ . After that we will plot the posterior probability distribution function (PDF) for  $H_0$ .

To compare our fit with the Planck data, we will plot  $d_L^{\text{obs}}(z_i)$  together with  $d_L^{\text{fit}}(z)$  and  $d_L^{\text{Planck}}(z)$ . We do this by computing the background with  $h, \Omega_{m0}, \Omega_{k0}$  replaced with the values of  $\hat{h}, \hat{\Omega}_{m0}, \text{okest}$  corresponding to  $\chi_{\text{min}}^2$ .

**Explain:  $\Omega_{b0} = 0.05$ , splining, etc...**

## 2.3. Results

In this section we present the results from our numerical simulations. Most of our results concern the evolution of various parameters as a function of  $x$ . Whenever it's relevant for interpreting and understanding the plot, we mark the point where we have matter-radiation equality and matter-dark energy equality, corresponding to  $\Omega_m = \Omega_r$  and  $\Omega_m = \Omega_{\Lambda}$ , respectively. These points can be seen directly in Fig. 5.

### 2.3.1. Analytical comparisons (Working title)

The dimensionless quantity  $\eta\mathcal{H}/c$  is shown in Fig. 1. At the lowest values of  $x \lesssim -10$ , we see that  $\eta\mathcal{H}/c = 1$ , as expected. Slightly before matter-radiation equality takes place, we see a slight increase towards higher  $x$ . As we approach higher  $x$ ,  $\Omega_{\Lambda}$  starts dominating, and the solution eventually diverges, as expected. **(Comment/derive expression for matter domination?)**.

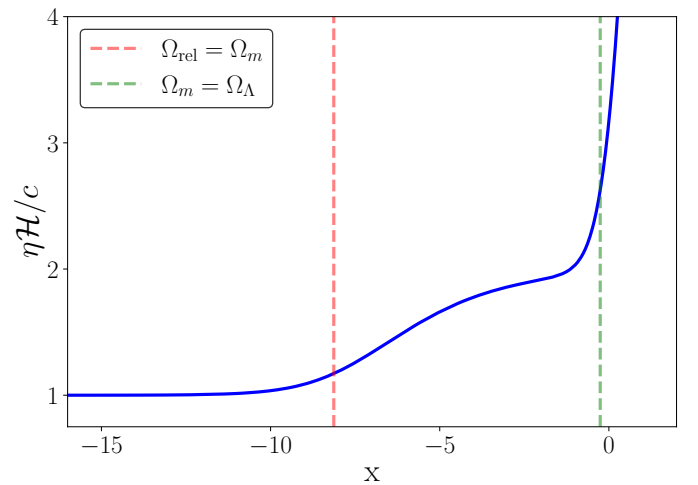


**Fig. 1.** Caption

In Fig. 2 we have plotted  $\mathcal{H}'/\mathcal{H}$  and  $\mathcal{H}''/\mathcal{H}$ , where we include the analytical approximation from (28) and (29), respectively. The different values of  $w$  are drawn over the whole range of  $x$  where their related density parameter is larger than the other two. This is done for visibility purposes, and we only expect approximations to be reasonable whenever a density parameter is close to 1.

Towards the smallest values of  $x$  we see that both quantities are well approximated by the analytical solutions for  $w = 1/3$ . As we reach  $x \gtrsim 12$ , matter becomes increasingly dominant, and the solution deviates from being purely dominated by a  $w = 1/3$  fluid. Towards the highest values of  $x$ , we see that both quantities reach a constant value of 1 for  $w = -1$ . At higher values of  $x$ , we know that both  $\Omega_m(x)$  and  $\Omega_r(x)$  should vanish, eventually, while  $\Omega_\Lambda \rightarrow 1$ . This behaviour is thus present in our implementation. When matter is the dominating constituent, we see that neither of the two functions are well approximated by a single fluid with  $w = 0$  as its equation of state parameter. This can be understood from Fig. 5, where the vanishing contribution of  $\Omega_r$  occurs around the same time as  $\Omega_\Lambda$  starts contributing. The maximum value reached is  $\Omega_m \approx 0.995$ . Nonetheless, the deviations are relatively small, and since  $\Omega_m = 1$  is never reached, it's reasonable to assume that our implementations are correct.

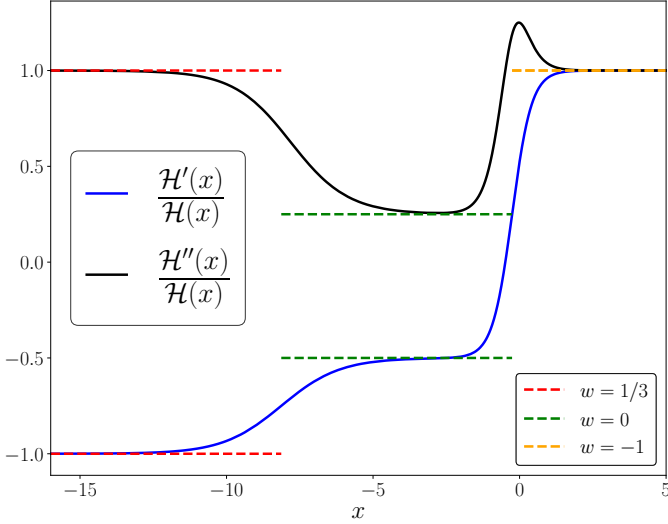


Fig. 2. Caption

### 2.3.2. Background evolution (working title)

Having checked that our implementation is physical, we now proceed by studying the evolution of the background, starting with a plot of the conformal Hubble factor,  $\mathcal{H}(x)$ , shown in Fig. 3.

The local minima taking place before matter-dark energy equality corresponds to the onset of acceleration, where  $\ddot{a} = 0$ . For  $x > 0$ ,  $\Omega_\Lambda$  will dominate the conformal Hubble factor, where we have  $\mathcal{H}(x) \propto e^x$ , as seen from Eq. (7).

The evolution of  $\eta(x)$  and  $t(x)$  is shown in Fig. 4. At high values of  $x$ , the  $e^x$  dependence of  $\mathcal{H}(x)$  causes  $\eta(x)$  to grow as  $e^{-x}$  at late times, suppressing its growth. The cosmic time, on the other hand, does not have an exponential dependence in the integrand at high values of  $x$ . This yields the linear growth we see at late times. The different  $x$ -dependence of  $t$  and  $\eta$  results in the two quantities to be approximately equal at  $x \sim 2.75$ .

Include log-plot at early times?

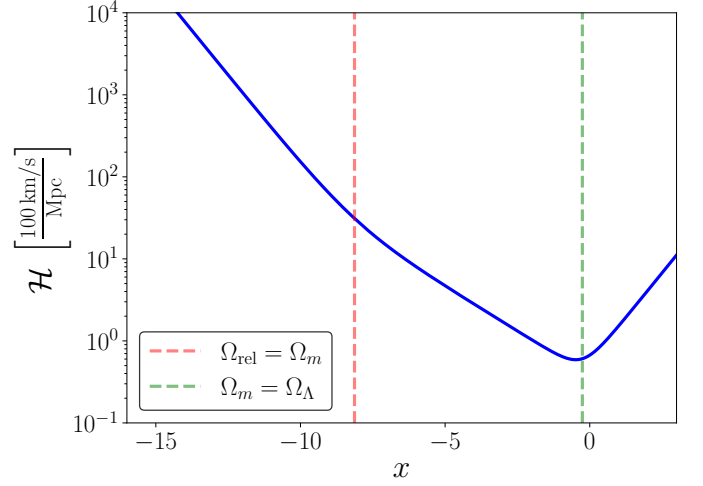


Fig. 3. hp

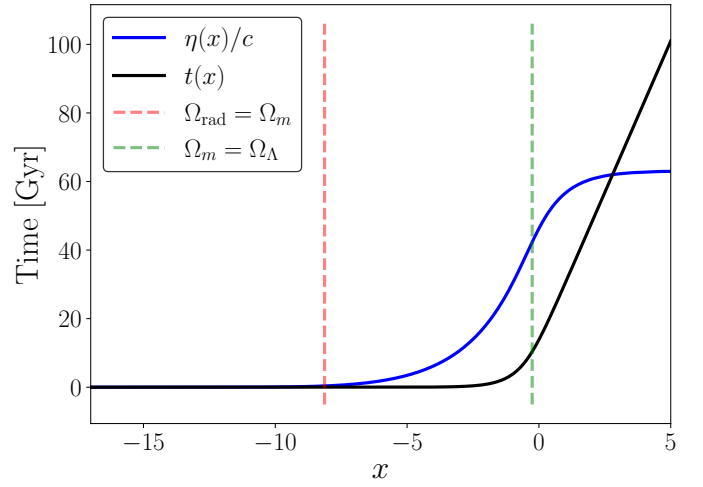


Fig. 4. times

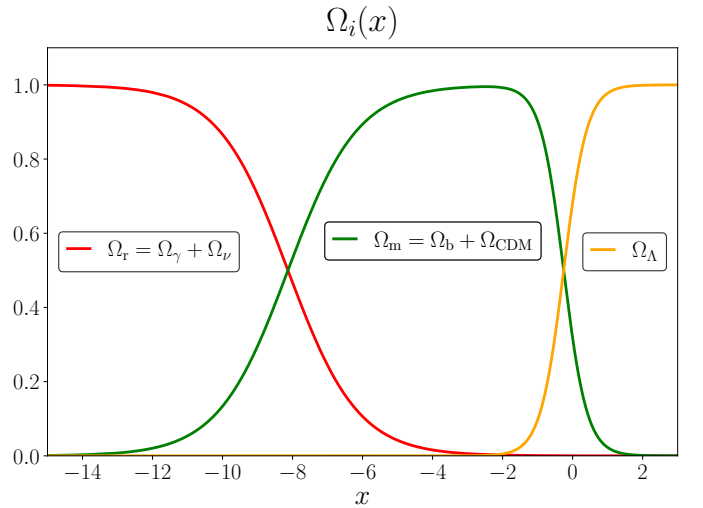


Fig. 5. Omegas

### 2.3.3. Supernova fitting

A plot showing the luminosity distance as a function of redshift is shown in Fig. 6, where we plot  $d_L(z)/z$  to better resolve the

details (details?). There is a noticeable discrepancy between the simulated luminosity distance and the data.

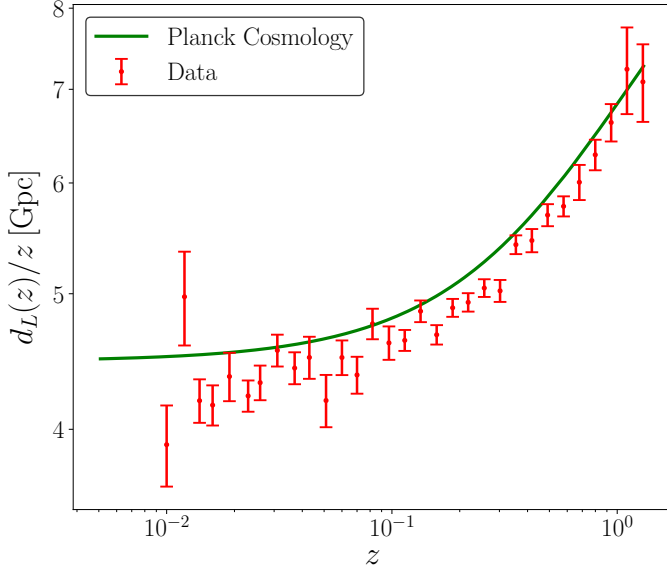


Fig. 6. dlz

The  $1\sigma$  and  $2\sigma$  confidence regions in the  $\Omega_\Lambda - \Omega_m$  plane is shown in Fig. 7. In the figure we have also indicated the parameter configuration for a flat Universe. A majority of the configurations seem to favour a non-flat Universe, but rather an **open** Universe, with  $\Omega_{k0} \approx 0.0674$ .

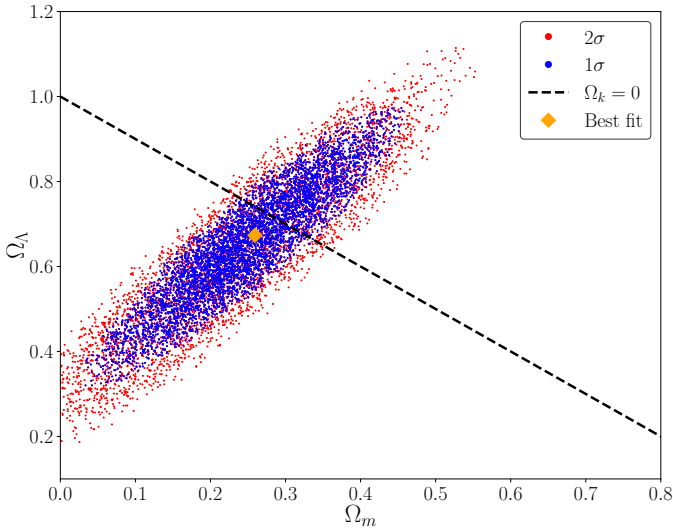


Fig. 7. plane

The posterior PDF of  $H_0$  is shown in Fig. 8, where we have included the resulting Gaussian distribution from the mean and variance of the sampled  $H_0$  values. This shows further discrepancy from the value of  $H_0 = 67$  [km/s/Mpc], given by Planck, while the mean value we obtain is  $\hat{H}_0 = 70.1$  [km/s/Mpc], with a corresponding standard deviation of  $\hat{\sigma}_{H_0} = 0.64$  [km/s/Mpc].

With the fitted parameters, we can solve the background cosmology once again, and compute the resulting luminosity distance

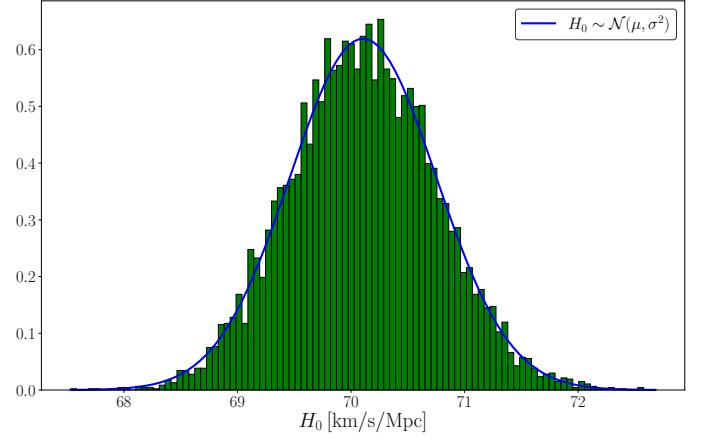


Fig. 8. pdf

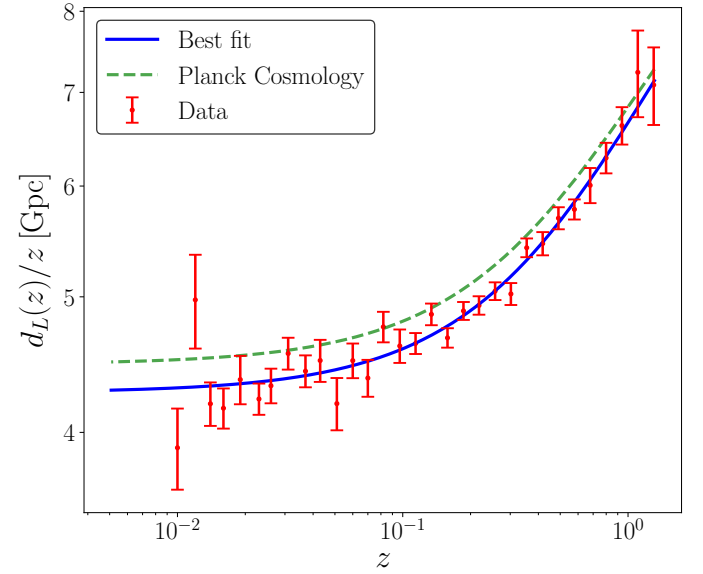


Fig. 9. dlz

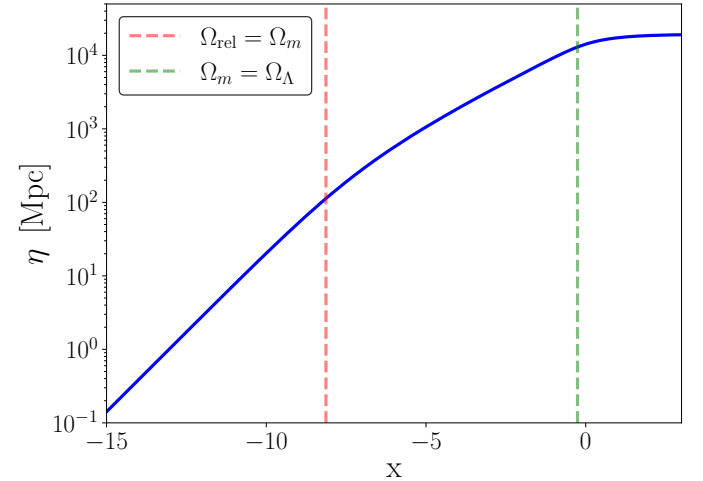


Fig. 10. REMOVE?

	$\Omega_m = \Omega_r$	$\Omega_m = \Omega_\Lambda$	$\ddot{a} = 0$	$t_0$	$\eta_0/c$
$x$	-8.13	-0.26	-0.49	13.85	46.29
$z$	3400.32	0.29	0.63	13.85	46.29
$t$ [Gyr]	51028.91 [yr]	10.37	7.75	13.85	46.29

### 3. Milestone II

Some introduction about what it is all about. And more so that

#### 3.1. Theory

The theory behind this milestone.

#### 3.2. Implementation details

Something about the numerical work.

#### 3.3. Results

Show and discuss the results.

### 4. Milestone III

Some introduction about what it is all about.

#### 4.1. Theory

The theory behind this milestone.

#### 4.2. Implementation details

Something about the numerical work.

#### 4.3. Results

Show and discuss the results.

### 5. Milestone IV

Some introduction about what it is all about.

#### 5.1. Theory

The theory behind this milestone.

#### 5.2. Implementation details

Something about the numerical work.

#### 5.3. Results

Show and discuss the results.

### 6. Conclusions

Write a short summary and conclusion in the end.

*Acknowledgements.* I thank my mom for financial support!

### References

- [1] Planck Collaboration, N. Aghanim, Y. Akrami, M. Ashdown, J. Aumont, C. Bacigalupi, M. Ballardini, A. J. Banday, R. B. Barreiro, N. Bartolo, S. Basak, R. Battye, K. Benabed, J. P. Bernard, M. Bersanelli, P. Bielewicz, J. J. Bock, J. R. Bond, J. Borrill, F. R. Bouchet, F. Boulanger, M. Bucher, C. Burigana, R. C. Butler, E. Calabrese, J. F. Cardoso, J. Carron, A. Challinor, H. C. Chiang, J. Chluba, L. P. L. Colombo, C. Combet, D. Contreras, B. P. Crill, F. Cuttaia, P. de Bernardis, G. de Zotti, J. Delabrouille, J. M. Delouis, E. Di

Valentino, J. M. Diego, O. Doré, M. Douspis, A. Ducout, X. Dupac, S. Dusini, G. Efstathiou, F. Elsner, T. A. Enßlin, H. K. Eriksen, Y. Fantaye, M. Farhang, J. Fergusson, R. Fernandez-Cobos, F. Finelli, F. Forastieri, M. Frailis, A. A. Fraisse, E. Franceschi, A. Frolov, S. Galeotta, S. Galli, K. Ganga, R. T. Génova-Santos, M. Gerbino, T. Ghosh, J. González-Nuevo, K. M. Górski, S. Gratton, A. Gruppuso, J. E. Gudmundsson, J. Hamann, W. Handley, F. K. Hansen, D. Herranz, S. R. Hildebrandt, E. Hivon, Z. Huang, A. H. Jaffe, W. C. Jones, A. Karakci, E. Keihänen, R. Keskitalo, K. Kiiveri, J. Kim, T. S. Kisner, L. Knox, N. Krachmalnicoff, M. Kunz, H. Kurki-Suonio, G. Lagache, J. M. Lamarre, A. Lasenby, M. Lattanzi, C. R. Lawrence, M. Le Jeune, P. Lemos, J. Lesgourgues, F. Levrier, A. Lewis, M. Liguori, P. B. Lilje, M. Lilley, V. Lindholm, M. López-Caniego, P. M. Lubin, Y. Z. Ma, J. F. Macías-Pérez, G. Maggio, D. Maino, N. Mandolesi, A. Mangilli, A. Marcos-Caballero, M. Maris, P. G. Martin, M. Martinelli, E. Martínez-González, S. Matarrese, N. Mauri, J. D. McEwen, P. R. Meinhold, A. Melchiorri, A. Mennella, M. Migliaccio, M. Millea, S. Mitra, M. A. Miville-Deschênes, D. Molinari, L. Montier, G. Morgante, A. Moss, P. Natoli, H. U. Nørgaard-Nielsen, L. Pagano, P. Paoletti, B. Partridge, G. Patanchon, H. V. Peiris, F. Perrotta, V. Pettorino, F. Piacentini, L. Polastri, G. Polenta, J. L. Puget, J. P. Rachen, M. Reinecke, M. Remazeilles, A. Renzi, G. Rocha, C. Rosset, G. Roudier, J. A. Rubiño-Martín, B. Ruiz-Granados, L. Salvati, M. Sandri, M. Savelainen, D. Scott, E. P. S. Shellard, C. Sirignano, G. Sirri, L. D. Spencer, R. Sunyaev, A. S. Suur-Uski, J. A. Tauber, D. Tavagnacco, M. Tenti, L. Toffolatti, M. Tomasi, T. Trombetti, L. Valenziano, J. Valiviita, B. Van Tent, L. Vibert, P. Vielva, F. Villa, N. Vittorio, B. D. Wandelt, I. K. Wehus, M. White, S. D. M. White, A. Zacchei, and A. Zonca. Planck 2018 results. VI. Cosmological parameters. *A&A*, 641:A6, September 2020. .

- [2] M. Betoule, R. Kessler, J. Guy, J. Mosher, D. Hardin, R. Biswas, P. Astier, P. El-Hage, M. König, S. Kuhlmann, J. Marriner, R. Pain, N. Regnault, C. Balleland, B. A. Bassett, P. J. Brown, H. Campbell, R. G. Carlberg, F. Cellier-Holzem, D. Cinabro, A. Conley, C. B. D’Andrea, D. L. DePoy, M. Doi, R. S. Ellis, S. Fabbro, A. V. Filippenko, R. J. Foley, J. A. Frieman, D. Fouchez, L. Galbany, A. Goobar, R. R. Gupta, G. J. Hill, R. Hlozek, C. J. Hogan, I. M. Hook, D. A. Howell, S. W. Jha, L. Le Guillou, G. Leloudas, C. Lidman, J. L. Marshall, A. Möller, A. M. Mourão, J. Neveu, R. Nichol, M. D. Olmstead, N. Palanque-Delabrouille, S. Perlmutter, J. L. Prieto, C. J. Pritchett, M. Richmond, A. G. Riess, V. Ruhlmann-Kleider, M. Sako, K. Schahmanee, D. P. Schneider, M. Smith, J. Sollerman, M. Sullivan, N. A. Walton, and C. J. Wheeler. Improved cosmological constraints from a joint analysis of the SDSS-II and SNLS supernova samples. *A&A*, 568:A22, August 2014. .
- [3] Scott Dodelson and Fabian Schmidt. *Modern Cosmology*. Academic Press, 2020. .

## **Appendix A: Bruh**

wewe

## **Appendix B: sis**